

# Electric field gradients in the rare earth–aluminium compounds $RAI_2$ and $RAI_3$ studied by $^{111}\text{Cd}$ perturbed angular correlations

M. Forker\* and P. de la Presa†

*Helmholtz Institut für Strahlen und Kernphysik der Universität Bonn, Nussallee 14-16, D-53115 Bonn, Germany*

(Received 8 March 2007; revised manuscript received 12 June 2007; published 12 September 2007)

Perturbed angular correlation (PAC) spectroscopy has been used to investigate the electric field gradient (EFG) at the probe nucleus  $^{111}\text{In}/^{111}\text{Cd}$  in the paramagnetic phase of the rare earth ( $R$ )–aluminium compounds  $RAI_2$  for all  $R$  elements and  $Y$  and in  $RAI_3$  for  $R=\text{Gd}, \text{Tm}, \text{Yb}, \text{Lu}$ . The nuclear electric quadrupole interaction (QI) between the EFG and the  $^{111}\text{Cd}$  quadrupole moment was measured as a function of temperature in the range  $T_C < T \leq 1200$  K. In the second half of the  $RAI_2$  series and in the  $RAI_3$  compounds, except for  $\text{YbAl}_3$ , the quadrupole frequency  $\nu_q$  shows the monotonous decrease with increasing temperature normally observed with closed-shell probe nuclei in metallic systems. In the early members of the  $RAI_2$  series, however,  $\nu_q(T)$  passes through a maximum at  $T \sim 300$  K. It is proposed that this unusual behavior reflects a contribution of the  $4f$  shell of the  $R$  constituents to the EFG at the Al site which is quenched at higher temperatures by thermal averaging of the  $4f$  quadrupole moment. In the intermediate-valence compound  $\text{YbAl}_3$  the temperature dependence of the QI exhibits a shallow maximum which can be related to the temperature variation of the  $4f$  hole occupation. Furthermore the PAC spectra provide information on the site preference of the  $^{111}\text{In}$  solutes in  $RAI_2$  for different  $R$  constituents and temperatures. In two-phase samples containing  $RAI_2$  and  $RAI_3$  with  $\text{AuCu}_3$  structure, at  $T < 900$  K the solutes show a very pronounced preference for the Al site of  $RAI_3$ , but at higher temperatures they migrate to the Al site of  $RAI_2$ . Jumps of the  $^{111}\text{In}/^{111}\text{Cd}$  probes on the Al sublattice of  $RAI_3$  compounds with  $\text{AuCu}_3$  structure ( $R=\text{Tm}, \text{Yb}, \text{Lu}$ ) lead to nuclear spin relaxation of  $^{111}\text{Cd}$ . The temperature dependence of the relaxation rates shows an Arrhenius behavior with jump activation enthalpies  $E_A = 1.6(1)$  eV for  $R=\text{Tm}, \text{Lu}$  and  $E_A = 1.2(1)$  eV for  $R=\text{Yb}$ .

DOI: 10.1103/PhysRevB.76.115111

PACS number(s): 71.20.Eh, 76.80.+y, 76.60.Es, 66.30.-h

## I. INTRODUCTION

Measurements of magnetic and electric hyperfine interactions (HFIs) of suitable probe nuclei may provide valuable information on the properties of intermetallic compounds.<sup>1,2</sup> Magnetic hyperfine interactions reflect the spin polarization, electric quadrupole interactions (QIs) the charge distribution surrounding the probe nucleus. We are presently engaged in a comprehensive perturbed angular correlation (PAC) study of magnetic and electric HFIs of non-rare-earth solutes in intermetallic compounds of the rare earths La to Lu. Recently, we have investigated<sup>3,4</sup> indirect exchange, anisotropic spin polarization, and crystal field parameters in magnetically ordered rare earth ( $R$ ) dialuminides  $RAI_2$  by measurement of the magnetic hyperfine field at the nuclear probe  $^{111}\text{Cd}$ .

In the present paper, we report an extension of this project to the electric quadrupole interaction between the  $^{111}\text{Cd}$  quadrupole moment and the electric field gradient (EFG) in the paramagnetic phase of the C15 Laves phases  $RAI_2$ . Mishra *et al.*<sup>5</sup> have reported the values of the room temperature EFG at  $^{111}\text{Cd}$  on the axial Al site of various rare earth dialuminides  $RAI_2$ . We have extended the measurements of Mishra *et al.*<sup>5</sup> to the entire  $RAI_2$  series and determined the temperature dependence of the QI of  $^{111}\text{Cd}$  in  $RAI_2$  for all trivalent  $R=\text{La} \cdots \text{Lu}$  and  $Y$ . (Note: For a recent overview of the binary rare earth Laves phases see Ref. 6).

One of the questions addressed by these measurements concerns the influence of the  $4f$  electrons on the EFG at nuclei on near-neighbor sites in metallic systems. Although the  $4f$  electrons are well shielded by the outer  $5d$  and  $6s$

electrons, there are indications<sup>7</sup> that their nonspherical charge distribution affects the EFG at near-neighbor positions and it has been pointed out by Rasera *et al.*<sup>8</sup> that such an influence might show up in the temperature dependence of the EFG.

The measurements also provide some information on the valence of the  $R$  constituents and evidence for temperature-induced changes of the site occupation of the  $^{111}\text{In}/^{111}\text{Cd}$  solutes from the noncubic Al site to the cubic  $R$  site of the C15 lattice of  $RAI_2$ . Temperature and composition driven changes of the site occupation of  $^{111}\text{In}$  in  $R$ -Al and Ni-Al phases and two-phase mixtures of Pd-Ga and Fe-Al intermetallic compounds have recently been reported by Collins and co-workers.<sup>9-11</sup> Similar studies for  $^{111}\text{In}$  and  $^{181}\text{Ta}$  in Hf and Zr dialuminides are due to Wodniecki *et al.*<sup>12</sup>

In samples of  $\text{TmAl}_2$  and  $\text{YbAl}_2$  containing minute amounts of the corresponding  $RAI_3$  compound we found an extreme preference of the  $^{111}\text{In}$  solutes for the Al site of  $RAI_3$  over that of  $RAI_2$ . This observation motivated an extension of the measurements to the QI of  $^{111}\text{Cd}$  in the trivalent  $RAI_3$ ,  $R=\text{Tm}, \text{Yb}, \text{Lu}$  which crystallize in the cubic  $\text{AuCu}_3$  structure. In this part of the study we compare the temperature variation of the EFG in  $\text{YbAl}_3$  to that in its neighbors  $\text{TmAl}_3$  and  $\text{LuAl}_3$ .  $\text{YbAl}_3$  exhibits intermediate-valence behavior<sup>13,14</sup> with a temperature variation of the  $4f$  hole occupation number resulting from the near degeneracy of the trivalent  $4f^{13}$  and the divalent  $4f^{14}$  configuration, whereas in  $\text{TmAl}_3$  and  $\text{LuAl}_3$  the  $R$  constituents are trivalent.

Time-dependent QIs caused by diffusion jumps of the  $^{111}\text{Cd}$  probes on the Al sublattice were observed in  $RAI_3$ ;  $R=\text{Tm}, \text{Yb}, \text{Lu}$  at  $T > 800$  K. The activation enthalpies of the

diffusion jumps were derived from the temperature dependence of the resulting nuclear spin relaxation.

## II. EXPERIMENTAL DETAILS

### A. Sample preparation and equipment

The compounds were prepared by arc melting of the metallic components in an argon atmosphere. Samples of  $RAI_2$  with the stoichiometry ratio 1:2 were produced for the rare earth constituents  $R=La, Ce, Pr, Nd, Sm, Eu, Gd, Tb, Dy, Ho, Er, Tm, Yb, Lu,$  and  $Y$ . Only samples for which the weight loss by melting was less than 1% were studied. The samples were characterized by x-ray diffraction. In all cases, the x-ray pattern confirmed the C15 structure with lattice parameter in agreement with the values reported in the literature. It is important to stress that contributions of other phases of the  $R$ -Al system, especially of  $RAI_3$ , were at the limit of detection ( $\leq 5\%$ ). In the case of  $EuAl_2$ , a small contribution of  $EuAl_4$  was present.<sup>15,16</sup>

For the identification of surprisingly high frequencies observed in  $RAI_2$  at the end of the  $R$  series ( $R=Tm$  and  $Yb$ ) the investigation of the  $^{111}Cd$  QI was extended to some  $RAI_3$  compounds. Within this series the structure varies with the  $R$  constituent: For  $R=Tm, Yb,$  and  $Lu$ ,  $RAI_3$  compounds crystallize in the  $AuCu_3$  structure. The  $SnNi_3$  structure is found for  $R=Ce, Pr, Gd$  and the  $BaPb_3$  structure for  $R=Tb, Y$ . (Note: Recently, Tsvyashchenko *et al.*<sup>17</sup> have shown that different structures may result when the compounds are synthesized under high pressure). X-ray diffraction measurements established that the  $RAI_3$  compounds of main interest in the context of our study ( $R=Tm, Yb,$  and  $Lu$ ) were almost single phase with contributions of  $RAI_2$  not exceeding 15%.

The 171–245 keV PAC cascade of  $^{111}Cd$  is populated by the electron capture decay of the  $2.8d$  isotope  $^{111}In$ . The intermediate state of the cascade has a half-life of  $T_{1/2}=84$  ns; its spin is  $I=5/2$ . The samples were doped with  $^{111}Cd$  by diffusion in vacuum (800 °C, 12 h) of carrier-free radioactive  $^{111}In$  into the host lattice.

The PAC measurements were carried out with a standard four-detector  $BaF_2$  setup in the temperature range  $10\text{ K} \leq T \leq 1273\text{ K}$ . Temperatures  $T < 290\text{ K}$  were obtained with a closed-cycle He refrigerator, whereas temperatures  $T > 290\text{ K}$  were produced with an especially designed PAC furnace.<sup>18</sup> For the high temperature measurements, the samples were encapsulated under vacuum into small quartz tubes.

### B. Data analysis

The modulation in time of a  $\gamma$ - $\gamma$  angular correlation by a static electric quadrupole interaction between the electric quadrupole moment  $Q$  of the intermediate state and an electric field gradient acting at the nuclear site can be described by the perturbation factor<sup>19</sup>

$$G_{kk}(t; \nu_q, \eta, \delta) = s_{k0} + \sum_n s_{kn} \cos(\omega_n t) \exp(-1/2 \delta \omega_n t). \quad (1)$$

The hyperfine frequencies  $\omega_n$  are related to the energy differences of the hyperfine levels into which the nuclear state is split by the QI. These frequencies depend on the

quadrupole frequency  $\nu_q = eQV_{zz}/h$  and the asymmetry parameter  $\eta = (V_{xx} - V_{yy})/V_{zz}$  where  $V_{ii} = \delta^2 V / \delta i^2$  ( $i=x, y, z$ ) are the principal-axis components of the EFG tensor with  $|V_{xx}| \leq |V_{yy}| \leq |V_{zz}|$ . In polycrystalline samples the amplitudes  $s_{kn}$  are functions of  $\eta$  only. The number  $n$  of terms in Eq. (1) depends on the spin of the nuclear state under consideration. For  $I=5/2$  one has  $n=3$ . The exponential factor accounts for possible distributions of the static QI caused by structural or chemical defects, which lead to an attenuation of the oscillatory PAC pattern. The parameter  $\delta$  is the relative width of a Lorentzian distribution.

When several fractions of nuclei subject to different hyperfine interactions are found in the same sample, the effective perturbation factor is given by

$$G_{kk}(t) = \sum_i f_i G_{kk}^i(t). \quad (2)$$

$f_i$  (with  $\sum_i f_i = 1$ ) is the relative intensity of the  $i$ th fraction. For sites with vanishing QI the angular correlation is unperturbed and one has  $G_{kk}(t) = 1$ .

In the present investigation both static and time-dependent EFGs were observed. Time-dependent QIs in solids are in many cases the result of atomic motion. The effect of the nuclear spin relaxation caused by jumping atoms on the angular correlation is most appropriately described by Blume's stochastic theory.<sup>20,21</sup> For the analysis of the dynamic perturbations observed in  $RAI_3$ , we have used an approximation of the Blume theory with a single relaxation parameter  $\lambda_k$  as follows:

$$G_{kk}(t) = \Gamma_{kk}(t) \exp(-\lambda_k t). \quad (3)$$

The validity of this approximation, the form of the function  $\Gamma_{kk}(t)$ , and the relation between the relaxation parameter  $\lambda_k$  and the jump rate  $w$  are discussed in Refs. 22 and 23.

## III. MEASUREMENTS AND RESULTS

### A. Quadrupole interactions of $^{111}Cd$ in $RAI_2$

Figure 1 presents the room temperature (RT) PAC spectra of  $^{111}Cd$  in  $RAI_2$  for  $R=La, Sm, Eu, Gd, Tb,$  and in  $YAl_2$ . The spectra show the periodic modulation of the anisotropy with time characteristic for an axially symmetric QI. The quadrupole frequencies were extracted by fitting Eq. (1) to the measured spectra. In all cases the asymmetry parameter was  $\eta \leq 0.05$ , the width of the Lorentzian frequency distribution  $\delta \leq 0.02$ . The RT values of the quadrupole frequencies listed in Table I agree with those reported by Mishra *et al.*<sup>5</sup> Except for  $EuAl_2$ , up to  $R=Tb$  the measured spectra could be reproduced by a single fraction implying that all probe nuclei reside on the axial Al site.

In the case of  $EuAl_2$  one observes a slowly decreasing anisotropy which shows that here the QI is much weaker than in the other  $RAI_2$ . By taking PAC spectra of  $^{111}Cd$  in  $EuAl_4$ , the fast oscillation of small amplitude superimposed on the weak decay of  $EuAl_2$  could be identified as an admixture of  $EuAl_4$ . The QI of  $^{111}Cd$  in  $EuAl_4$  is axially symmetric ( $\nu_q = 89.3$  MHz,  $\eta = 0$  at 300 K), consistent with the body centered tetragonal  $BaAl_4$  structure type.<sup>15,16</sup> Although there are two Al sites<sup>24</sup> in  $EuAl_4$  we observed a single, well-

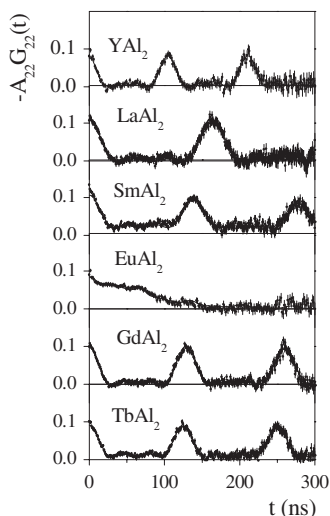


FIG. 1. Room temperature PAC spectra of  $^{111}\text{Cd}$  in the Laves phases  $\text{YAl}_2$  and  $\text{RAl}_2$ .

defined quadrupole frequency ( $\delta \leq 0.02$ ) which suggests a pronounced preference of the  $^{111}\text{In}/^{111}\text{Cd}$  solutes for one of these sites.

The  $^{111}\text{Cd}$  PAC spectra at the end of the  $\text{RAl}_2$  series (see Fig. 2) differ from those in the earlier members in two aspects:

(i) There is a tendency toward occupation of the cubic  $R$  site which becomes manifest in a vertical shift and reduced amplitude of the periodic modulation (see the spectra of  $\text{R}_{1.03}\text{Al}_2$ ,  $R=\text{Dy}, \text{Er}, \text{Tm}, \text{Yb}, \text{Lu}$  in Fig. 2). This tendency is most pronounced at the end of the  $R$  series: In *stoichiometric*  $\text{LuAl}_2$ , the PAC spectrum at 300 K showed a slow decrease of the anisotropy with—if at all—only a very small periodic modulation indicating that practically all probe nuclei are subject to a frequency distribution centered close to frequency zero. This is clear evidence for the occupation of the cubic  $R$  site at which the QI is expected to vanish [perturbation factor  $G_{kk}^R(t)=1$ ]. The observation of a weak rather than zero QI can be attributed to nearby point defects.

TABLE I. Quadrupole frequency  $\nu_q$  of  $^{111}\text{Cd}$  in rare earth dialuminides  $\text{RAl}_2$ ;  $R=\text{Y}-\text{Tb}$  at 300 K.  $-\frac{\delta \ln \nu_q(T)}{\delta T}|_{400\text{ K}}$  is the coefficient of the linear temperature dependence at  $T \geq 400$  K.

Rare earth $R$	$\nu_q$ (MHz)	$-\frac{\delta \ln \nu_q(T)}{\delta T} _{400\text{ K}}$ ( $10^{-4} \text{ K}^{-1}$ )
Y	62.8 <sub>1</sub>	2.41 <sub>5</sub>
La	40.5 <sub>1</sub>	2.34 <sub>5</sub>
Ce	43.1 <sub>1</sub>	2.37 <sub>5</sub>
Pr	43.5 <sub>1</sub>	2.44 <sub>5</sub>
Nd	43.5 <sub>1</sub>	1.94 <sub>5</sub>
Sm	45.6 <sub>1</sub>	2.45 <sub>5</sub>
Eu	9 <sub>2</sub>	
Gd	50.9 <sub>1</sub>	1.90 <sub>5</sub>
Tb	53.5 <sub>1</sub>	2.19 <sub>5</sub>

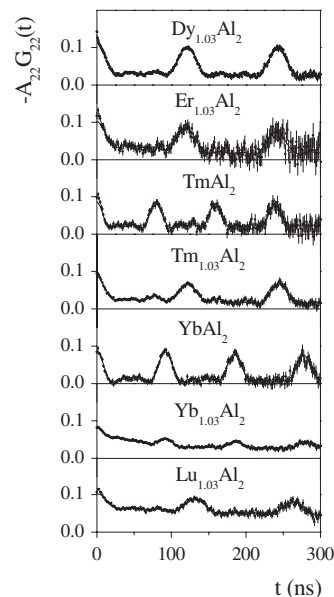


FIG. 2. Room temperature PAC spectra of  $^{111}\text{Cd}$  in  $\text{RAl}_2$  with heavy  $R$  constituents. For  $R=\text{Tm}$  and  $\text{Yb}$ , spectra of compounds with the exact stoichiometry and with a slight  $R$  excess, respectively, are shown.

The  $R$  site occupation could be reduced by allowing a slight  $R$  excess ( $\leq 3\%$ ). At the end of the  $\text{RAl}_2$  series, the temperature dependence of the QI of the Al site was therefore measured with samples of the composition  $\text{R}_{1.03}\text{Al}_2$ . The spectra were analyzed by allowing up to three components with different QI parameters. The quadrupole frequencies and fractions derived from the room temperature spectra of  $\text{R}_{1.03}\text{Al}_2$ ,  $R=\text{Dy}, \text{Ho}, \text{Er}, \text{Tm}, \text{Yb}, \text{Lu}$  are listed in Table II.

(ii) For  $R=\text{Tm}$  and  $\text{Yb}$ , the QI of  $^{111}\text{Cd}$  in stoichiometric  $\text{RAl}_2$  was found to be substantially stronger than expected from the variation of the quadrupole frequency with the  $R$  constituent (see Table I): For  $R=\text{Ho}, \text{Er}$  one has  $\nu_q = 55.7(2)$  MHz and one would expect a similar value at least for  $\text{TmAl}_2$ . The first measurements for  $R=\text{Tm}$  and  $\text{Yb}$ , however, gave RT frequencies of  $\nu_q \sim 83$  MHz and  $\nu_q \sim 71$  MHz, respectively, an increase—relative to  $\text{ErAl}_2$ —of almost 50% clearly visible in Fig. 2. For  $R=\text{Lu}$ , this high frequency component was not observed. By measurements of the QI of  $^{111}\text{Cd}$  in  $\text{RAl}_3$  (see Sec. III C) the high frequencies found in  $\text{RAl}_2$ ,  $R=\text{Tm}$  and  $\text{Yb}$  could be identified as those of the respective  $\text{RAl}_3$  compounds.

In the x-ray diffraction (XRD) pattern of stoichiometric  $\text{RAl}_2$ , contributions of  $\text{RAl}_3$  were barely detectable ( $\leq 5\%$ ). The relative intensities of the  $\text{RAl}_3$  frequencies in  $\text{TmAl}_2$  and  $\text{YbAl}_2$ , however, exceed 70% (see Table II) from which one may infer that—given the opportunity in two-phase samples— $^{111}\text{In}$  solutes strongly prefer  $\text{RAl}_3$  compounds with  $\text{AuCu}_3$  structure over the corresponding C15  $\text{RAl}_2$  Laves phases.

The  $\text{TmAl}_3$  component in the  $\text{TmAl}_2$  spectra could be strongly suppressed by a slight Tm excess (see Fig. 2). In  $\text{Tm}_{1.03}\text{Al}_2$ , only 16% of the probes experience the high  $\text{TmAl}_3$  frequency, but  $\sim 60\%$  are now subject to a frequency  $\nu_q = 54.8$  MHz which fits well into the trend of the QI ob-

TABLE II. The quadrupole frequencies  $\nu_q$  and fractions of different components found in the room temperature PAC spectra of  $^{111}\text{Cd}$  in  $R_{1+x}\text{Al}_2$  Laves phases with the heavy  $R$  constituents  $R=\text{Dy}-\text{Lu}$  and  $R$  excess in the range  $-0.005 \leq x \leq 0.03$ . The quantity  $-\frac{\delta \ln \nu_q(T)}{\delta T}|_{400 \text{ K}}$  is the coefficient of the linear temperature dependence at  $T \geq 400 \text{ K}$ .

Rare earth $R$	$R$ excess $x$	$\nu_q$ (MHz)	$-\frac{\delta \ln \nu_q(T)}{\delta T} _{400 \text{ K}}$ ( $10^{-4} \text{ K}^{-1}$ )	Fraction	Site
Dy	$-0.005 \leq x \leq 0.03$	$54.9_1$	$2.35_5$	$\geq 0.8$	Al of $R\text{Al}_2$
		$\leq 2$		$\leq 0.2$	$R$ of $R\text{Al}_2$
Ho	$-0.005 \leq x \leq 0.03$	$55.7_1$	$2.21_5$	$\geq 0.8$	Al of $R\text{Al}_2$
		$\leq 2$		$\leq 0.2$	$R$ of $R\text{Al}_2$
Er	$-0.005 \leq x \leq 0.03$	$55.8$	$1.93_7$	$\geq 0.7$	Al of $R\text{Al}_2$
		$\leq 2$		$\leq 0.3$	$R$ of $R\text{Al}_2$
Tm	$x=0.00$	$83.7_1$		0.71	Al of $\text{TmAl}_3$
		$54.6$		0.06	Al of $\text{TmAl}_2$
		$\leq 2$		0.23	$R$ of $\text{TmAl}_2/\text{TmAl}_3$
	$x=0.03$	$83.8_1$	$2.26_5$	0.16	Al of $\text{TmAl}_3$
		$54.8_1$		0.57	Al of $\text{TmAl}_2$
		$\leq 2$		0.27	$R$ of $\text{TmAl}_2/\text{TmAl}_3$
Yb	$x=0.00$	$71.8_1$		0.9	Al of $\text{YbAl}_3$
		$\leq 2$		0.1	$R$ of $\text{YbAl}_2/\text{YbAl}_3$
	$x=0.03$	$71.2_2$		0.28	Al of $\text{YbAl}_3$
		$11_2$		0.34	Al of $\text{YbAl}_2$
		$\leq 2$		0.38	$R$ of $\text{YbAl}_2/\text{YbAl}_3$
Lu	$x=0.03$	$50.2_3$	$2.30_5$	0.35	Al of $R\text{Al}_2$
		$\leq 2$		0.65	$R$ of $R\text{Al}_2$

served in trivalent  $R\text{Al}_2$  up to  $R=\text{Er}$ . Furthermore, there is a fraction (27%) of probes in an almost cubic ( $\nu_q \leq 2 \text{ MHz}$ ) environment.

In the case of  $\text{YbAl}_2$ ,  $R$  excess did not produce the  $\sim 55 \text{ MHz}$  component expected from the trend of the QI in  $R\text{Al}_2$  with trivalent  $R$  constituents. The spectrum of  $\text{Yb}_{1.03}\text{Al}_2$  (see Fig. 2) consists of three components: 28% of the probes show the 71 MHz precession of  $\text{YbAl}_3$ ,  $\sim 38\%$  with  $\nu_q \leq 2 \text{ MHz}$  account for the vertical offset, and a fraction of  $\sim 34\%$  subject to  $\sim 11 \text{ MHz}$  is required to describe the initial decrease of the anisotropy.

In Fig. 3 (bottom most section) we have collected the results of the analysis, attributing the 50–55 MHz components in the spectra of  $\text{Tm}_{1.03}\text{Al}_2$  and  $\text{Lu}_{1.03}\text{Al}_2$  to the  $R\text{Al}_2$  Laves phases. The  $R\text{Al}_2$  quadrupole frequencies are plotted versus the  $R$  atomic number.

The temperature dependence of the QI of  $^{111}\text{Cd}$  in  $R\text{Al}_2$  was measured in the range  $T_C < T \leq 1200 \text{ K}$ . The magnetic-order temperatures  $T_C$  of  $R\text{Al}_2$  vary between 3.85 K for  $\text{CeAl}_2$  and 168 K for  $\text{GdAl}_2$ . Figure 4 presents spectra of  $^{111}\text{Cd}$  in  $\text{PrAl}_2$  at different temperatures as a prominent example of the spectra of light  $R\text{Al}_2$ : The spin precession period has a minimum at  $\sim 300 \text{ K}$ , i.e., as one moves from 40 to 990 K, the quadrupole frequency passes through a maximum. This is quite unusual for a closed-shell probe atom in a metallic host. Usually one finds a monotonous

decrease of the QI with increasing temperature. The same behavior was observed in all  $R\text{Al}_2$  with light  $R=\text{La}$  to  $\text{Sm}$  (Fig. 5). The difference  $[\nu_q^{\text{max}} - \nu_q(T_C)]/\nu_q^{\text{max}}$ , with  $\nu_q^{\text{max}}$  the frequency maximum, varies from 0.073 for Pr, Ce to 0.02 for La, Nd, and 0.013 for Sm. At  $T \geq 400 \text{ K}$ ,  $\nu_q(T)$  follows a linear relation with slopes  $-d \ln \nu_q/dT|_{400 \text{ K}}$  listed in Table I. In heavy  $R\text{Al}_2$  and in  $\text{YAl}_2$ , the quadrupole frequency decreases monotonously with increasing temperature. The decrease is well described by straight lines with temperature coefficients given in Tables I and II.

### B. Temperature-induced changes of the site occupied by $^{111}\text{In}/^{111}\text{Cd}$ in $R\text{Al}_2$ and $R\text{Al}_3$

The observation of a single, axially symmetric QI indicates that in the early members of the  $R\text{Al}_2$  series the  $^{111}\text{In}$  solutes exclusively occupy the Al site at all temperatures. At the end of the series, however, one finds evidence for temperature-induced solute migration between different sites: The RT spectrum of  $\text{Tm}_{1.03}\text{Al}_2$  (see Fig. 2) contains the 54.8 MHz component of  $\text{TmAl}_2$  and 83.8 MHz component of  $\text{TmAl}_3$  with an intensity ratio of  $\sim 3:1$ . As temperature is increased, the PAC pattern changes reversibly (see Figs. 6 and 7): Up to  $T \leq 900 \text{ K}$ , the intensity of the  $\sim 80 \text{ MHz}$  component (precession period in Fig. 6:  $\sim 75 \text{ ns}$ ) grows at the expense of the  $\sim 50 \text{ MHz}$  component, but at still higher tem-

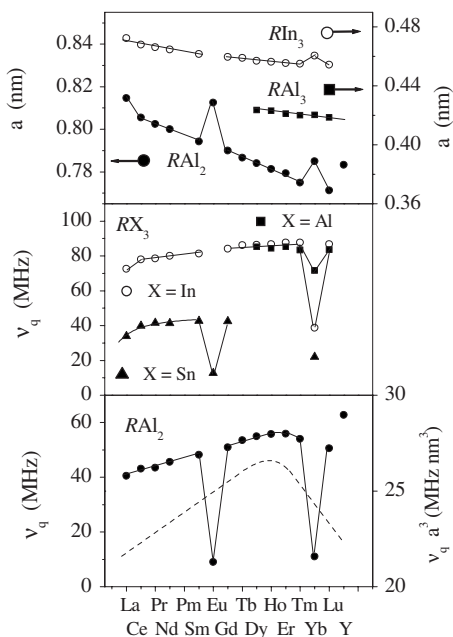


FIG. 3. The  $R$  dependence of the room temperature quadrupole frequency  $\nu_q$  of  $^{111}\text{Cd}$  in  $R\text{Al}_2$  and in  $RX_3$  compounds with  $\text{AuCu}_3$  structure. The  $R\text{Al}_3$  compounds ( $R=\text{Tm}, \text{Yb}, \text{Lu}$ ) studied in the present work were synthesized at atmospheric pressure, and those investigated by Tsvyashchenko *et al.* (Ref. 17) ( $R=\text{Dy}, \text{Ho}, \text{Er}, \text{Tm}, \text{Yb}, \text{Lu}$ ) at high pressures. The values for  $RX_3$ ;  $X=\text{In}, \text{Sn}$  have been reported by Schwartz and Shirley (Ref. 29) The topmost section shows the lattice parameter  $a$  of  $R\text{Al}_2$  (this work and Ref. 5),  $R\text{Al}_3$  (this work and Ref. 17), and  $R\text{In}_3$  (Ref. 29) at 300 K as a function of the  $R$  constituent. The dashed line in the bottom-most section corresponds to the quantity  $\nu_q a^3$  (right-hand scale) of  $R\text{Al}_2$  with trivalent  $R$  constituents.

peratures this component decreases continuously toward zero. In the quantitative least-squares fit analysis three sites were assumed: the Al site of  $\text{TmAl}_2$  with  $\nu_q \sim 50$  MHz, the Al site of  $\text{TmAl}_3$  with  $\nu_q \sim 80$  MHz, and a cubic site with  $\nu_q \sim 0$  MHz necessary to account for a slight vertical offset of the spectra. The temperature dependence of the relative

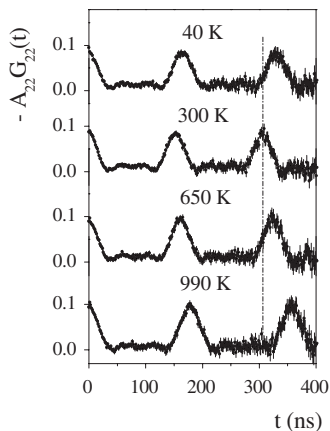


FIG. 4. PAC spectra of  $^{111}\text{Cd}$  in  $\text{PrAl}_2$  at different temperatures. The vertical line marks the time of two spin precessions at 300 K.

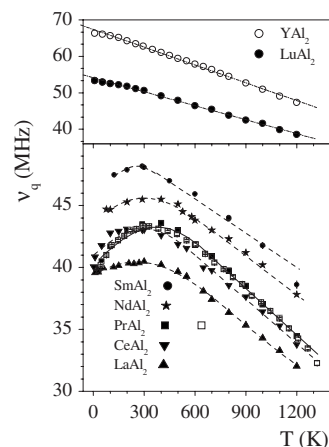


FIG. 5. Temperature dependence of the quadrupole frequency of  $^{111}\text{Cd}$  in  $R\text{Al}_2$  with light  $R$  constituents (lower section). The upper section presents the data of  $\text{LuAl}_2$  as a typical example of  $\nu_q(T)$  of heavy  $R\text{Al}_2$  and of  $\text{YAl}_2$ . (Note the difference in scale when comparing the slopes of light and heavy  $R$  for  $T > 400$  K.)

intensities of the  $\sim 50$  MHz and the  $\sim 80$  MHz components collected in Fig. 7 shows that at  $T < 900$  K some of the  $^{111}\text{In}$  solutes migrate from the  $\text{TmAl}_2$  to the  $\text{TmAl}_3$  grains of the sample, but at  $T > 900$  K the solutes clearly prefer to reside on the Al site of  $\text{TmAl}_2$ .

While the PAC spectra of  $\text{Tm}_{1.03}\text{Al}_2$  reflect solute migration between different phases present in the same sample, those of  $\text{Lu}_{1.03}\text{Al}_2$  (Fig. 8) provide an example for solute transfer between different sites of the same phase: The room temperature spectrum of  $\text{Lu}_{1.03}\text{Al}_2$  consists of the periodic modulation characteristic for probes on the axial Al site, superimposed on the slowly decaying anisotropy of probes on the cubic  $R$  site. Comparison of the 300 and 1100 K spectra in Fig. 8 shows that the relative occupation of the Al and  $R$  sites changes with temperature. The ratio  $f_{\text{Lu}}/f_{\text{Al}}$  ( $f_X$  = fraction of probes on site  $X$ ), determined from spectra in the range  $10\text{K} \leq T \leq 1200$  K, was constant up to  $T \leq 600$  K.

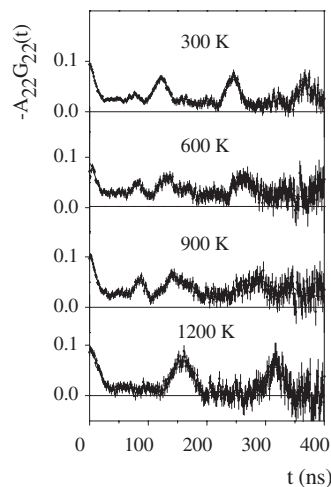


FIG. 6. PAC spectra of  $^{111}\text{Cd}$  in  $\text{Tm}_{1.03}\text{Al}_2$  at different temperatures.

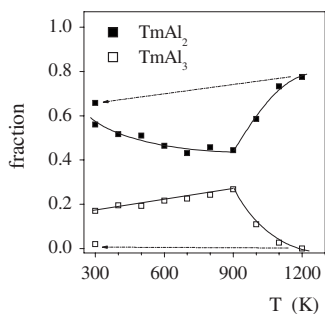


FIG. 7. The preference of the solute  $^{111}\text{In}/^{111}\text{Cd}$  for the Al site in  $\text{TmAl}_2$  (full squares) and  $\text{TmAl}_3$  (open squares), respectively, as a function of temperature.

At higher temperatures, it follows the relation  $f_{\text{Lu}}/f_{\text{Al}}(T) \propto \exp(H/k_B T)$  with  $H=0.25(2)$  eV where  $H$  is the change in enthalpy<sup>9</sup> due in the transfer of probes from the Lu to the Al site. At RT after 1200 K, all probes are found on the Lu site.

### C. Static and dynamic quadrupole interactions of $^{111}\text{Cd}$ in $\text{RAl}_3$ , $\text{R}=\text{Gd}, \text{Tm}, \text{Yb}, \text{Lu}$

To clarify the origin of the high quadrupole frequencies at the end of the  $\text{RAl}_2$  series, the PAC measurements were extended to the  $\text{RAl}_3$  compounds with  $\text{AuCu}_3$  structure ( $\text{R}=\text{Tm}, \text{Yb},$  and  $\text{Lu}$ ). Spectra of  $^{111}\text{Cd}$  in  $\text{LuAl}_3$  and  $\text{YbAl}_3$  are shown in Figs. 9 and 10, respectively. At  $T < 800$  K, we observed the periodic nonattenuated modulation characteristic for an axially symmetric QI. Line broadening by inhomogeneities was less than 2%, and contributions by other phases, especially  $\text{RAl}_2$ , were below the limit of PAC detection, although the XRD pattern of some  $\text{RAl}_3$  contained  $\text{RAl}_2$  reflections with an intensity of up to 15%.

We also studied  $\text{GdAl}_3$ , a  $\text{RAl}_3$  compounds with  $\text{SnNi}_3$  structure to see whether the dynamic interaction observed in  $\text{RAl}_3$ ,  $\text{R}=\text{Tm}, \text{Yb}, \text{Lu}$  (see below) occurs also in  $\text{RAl}_3$  compounds with other structures. The spectra of  $\text{GdAl}_3$  (not shown) present a single, slightly asymmetric static QI without indications of dynamic perturbations up to  $T \leq 1250$  K. The room temperature QI parameters derived by a fit of Eq. (1) to the experimental data are listed in Table III. The RT

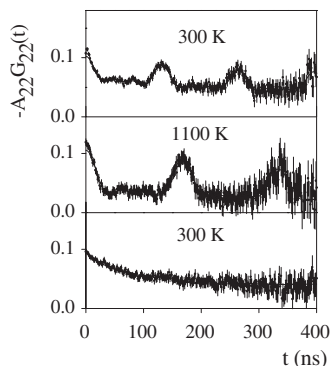


FIG. 8. PAC spectra of  $^{111}\text{Cd}$  in  $\text{Lu}_{1.03}\text{Al}_2$  at different temperatures.

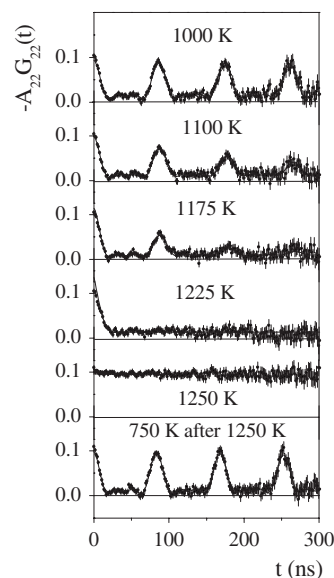


FIG. 9. PAC spectra of  $^{111}\text{Cd}$  in  $\text{LuAl}_3$  at high temperatures.

parameters of  $\text{GdAl}_3$  are in agreement with the previous result of Zacate and Collins,<sup>9</sup> the parameters of  $\text{RAl}_3$ ,  $\text{R}=\text{Tm}, \text{Yb}, \text{Lu}$  agree within 2% with the values recently reported by Tsvyashchenko *et al.*<sup>17</sup> for  $\text{RAl}_3$  compounds synthesized under high pressure.

The temperature dependencies of the quadrupole frequencies of  $^{111}\text{Cd}$  in  $\text{RAl}_3$ ,  $\text{R}=\text{Gd}, \text{Tm}, \text{Yb}, \text{Lu}$  are shown in Fig. 11. Except for  $\text{YbAl}_3$  where  $\nu_q(T)$  passes through a shallow maximum, one observes a monotonous decrease of  $\nu_q$  with increasing temperature. For  $\text{R}=\text{Gd}, \text{Tm},$  and  $\text{Lu}$ ,  $\nu_q(T)$  is a linear function in the range  $10 \text{ K} \leq T \leq 1200 \text{ K}$ . The temperature coefficients are listed in Table III. The  $\text{GdAl}_3$  asymmetry parameter decreases from  $\eta=0.20(1)$  at 10 K to  $\eta=0$  at  $T \geq 1000$  K.

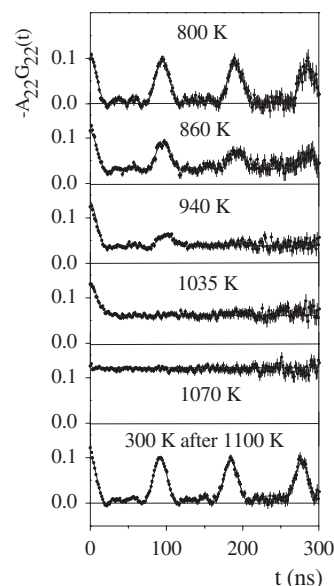


FIG. 10. PAC spectra of  $^{111}\text{Cd}$  in  $\text{YbAl}_3$  at high temperatures.

TABLE III. Quadrupole frequency  $\nu_q$ , the asymmetry  $\eta$ , and fractions of  $^{111}\text{Cd}$  in  $\text{RAl}_3$  compounds at 300 K. The linear temperature dependence of  $\nu_q$  at  $10\text{ K} \leq T \leq 1200\text{ K}$  is expressed by  $-\frac{\delta \ln \nu_q(T)}{\delta T} \Big|_{10\text{ K}}$ . In the case of  $\text{YbAl}_3$  the temperature coefficient for  $T > 400\text{ K}$  is given.

Rare earth $R$	Structure type	$\nu_q$ (MHz)	Asymmetry $\eta$	$-\frac{\delta \ln \nu_q(T)}{\delta T} \Big _{10\text{ K}}$ ( $10^{-4}\text{ K}^{-1}$ )
Gd	$\text{SnNi}_3$	$64.0_1$	$0.12_1$	$2.53_5$
Tm	$\text{AuCu}_3$	$83.5_1$	$\leq 0.05$	$0.81_4$
Yb	$\text{AuCu}_3$	$71.6_1$	$\leq 0.05$	$0.46_{12}$ ( $T > 400\text{ K}$ )
Lu	$\text{AuCu}_3$	$83.4_1$	$\leq 0.05$	$1.08_3$

At temperatures  $T > 800\text{ K}$ , the spectra of  $\text{RAl}_3$ ,  $R = \text{Tm, Yb, Lu}$  undergo pronounced, fully reversible changes, as illustrated in Figs. 9 and 10 for the case of  $\text{LuAl}_3$  and  $\text{YbAl}_3$ . As temperature is raised beyond  $1000\text{ K}$ , the periodic spin precessions of the spectra of  $\text{LuAl}_3$  and  $\text{TmAl}_3$  suffer an exponential attenuation which increases with temperature up to the complete disappearance of the oscillations at  $T \sim 1225\text{ K}$ : These are features of a perturbation by time-dependent interaction.<sup>20,21</sup> The high temperature ( $T > 1000\text{ K}$ ) spectra of  $\text{RAl}_3$ ,  $R = \text{Tm, Lu}$  were therefore analyzed using Eq. (3) with  $\Gamma_{kk}(t)$  given by the perturbation factor for a static QI [Eq. (2)]. The resulting relaxation parameters  $\lambda_2$  are collected in Fig. 12 in form of an Arrhenius plot  $\lambda_2(T) = \lambda_2^0 \exp(-E_A/k_B T)$  from which one obtains an activation enthalpy of the fluctuations of  $E_A = 1.6(1)\text{ eV}$  with prefactor  $\lambda_2^0 = (1_{-0.5}^{+1}) 10^{14}\text{ s}^{-1}$  for  $R = \text{Tm}$  and  $\text{Lu}$ .

At temperatures  $T > 1225\text{ K}$ , one expects the spectrum to evolve from maximum relaxation toward the limit of fast motional narrowing which—in case the fluctuating interaction has zero time average—is the unperturbed angular correlation. Figure 9 shows that the unperturbed correlation in  $\text{LuAl}_3$  is reached at  $T = 1250\text{ K}$ .

If the jump frequency  $w$  follows an exponential temperature dependence  $w = w_0 \exp(-E_A/k_B T)$  with attempt frequency  $w_0$ , an Arrhenius plot of the relaxation parameter  $\ln \lambda_2$  versus  $1/T$  should show the same slope (but opposite sign) in the region of slow [ $\lambda_k = \lambda_k^0 \exp(-E_A/k_B T)$ ] and fast fluctuations [ $\lambda_k = \lambda_k^0 \exp(E_A/k_B T)$ ], respectively. It is therefore surprising to find that in the case of  $\text{LuAl}_3$  and  $\text{TmAl}_3$  it

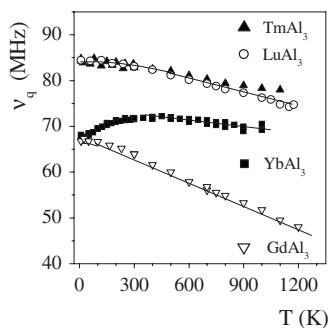


FIG. 11. Temperature dependence of the quadrupole frequency of  $^{111}\text{Cd}$  in some  $\text{RAl}_3$  compounds ( $R = \text{Gd, Tm, Yb, Lu}$ ).

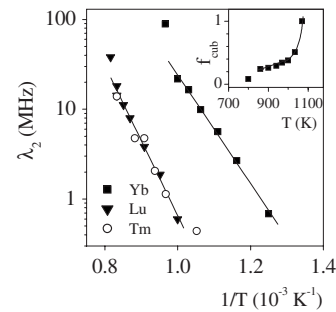


FIG. 12. Arrhenius plot of the relaxation parameter  $\lambda_2$  of  $^{111}\text{Cd}$  in  $\text{RAl}_3$  compounds ( $R = \text{Tm, Yb, Lu}$ ) with  $\text{AuCu}_3$  crystal structure. The insert shows the temperature dependence of the cubic fraction in the PAC spectra of  $\text{YbAl}_3$ .

takes a temperature increase of about  $200\text{ K}$  to completely attenuate the oscillations observed at  $T \leq 1000\text{ K}$ , but only  $25\text{ K}$  to go from total attenuation to unperturbed anisotropy.

In  $\text{YbAl}_3$  (Fig. 10) the attenuation of the periodic oscillations sets in at a lower temperature ( $T \geq 800\text{ K}$ ) than in  $\text{LuAl}_3$  and  $\text{TmAl}_3$  and together with the attenuation there is a vertical shift of the spectra which was not observed in the other two  $\text{RAl}_3$ . The shift implies the presence of two fractions of probes at  $T > 800\text{ K}$ , one subject to the fluctuating QI, and the other unperturbed in a cubic environment. Correspondingly, the spectra of  $\text{YbAl}_3$  were analyzed with a two-site model:  $G_{22}(t) = (1 - f_{\text{cub}}) \Gamma_{22}(t) \exp(-\lambda_2 t) + f_{\text{cub}}$ . The temperature dependence of the unperturbed fraction  $f_{\text{cub}}$  is shown in the insert of Fig. 12. For  $\text{YbAl}_3$  the activation enthalpy is  $E_A = 1.2(1)\text{ eV}$  and the prefactor  $\lambda_2^0 = (2.7_{-1.1}^{+1.7}) 10^{13}\text{ s}^{-1}$ .

## IV. DISCUSSION

### A. Site occupation, solute migration, and diffusion of $^{111}\text{In}/^{111}\text{Cd}$ in $\text{RAl}_2$ and $\text{RAl}_3$

The Al site of the  $\text{RAl}_2$  Laves phases has axial ( $3m$ ) symmetry with six nearest neighbor (NN) Al atoms at  $0.283(\text{Ce}) - 0.274(\text{Lu})\text{ nm}$ , the  $R$  site has cubic symmetry ( $43m$ ) with 12 NN Al atoms at  $0.332(\text{Ce}) - 0.322(\text{Lu})\text{ nm}$ . The observation of a single component with an axially symmetric QI therefore implies that at the beginning of the  $R$  series all  $^{111}\text{Cd}$  probes reside on the Al site. Toward the end of the series a cubic component appears in the PAC spectra, indicating the partial occupation of the  $R$  site.

The site chosen by an impurity atom in an intermetallic compound can be expected to depend on the differences in size and charge of the solute and the constituents of the intermetallic compound. The atomic radius of In ( $0.156\text{ nm}$ ; empirical Slater value<sup>25</sup>) is considerably larger than that of Al ( $0.125\text{ nm}$ ), but smaller than the  $R$  radii [ $0.195(\text{Ce}) - 0.175(\text{Lu})\text{ nm}$ ]. The fact that in light  $\text{RAl}_2$   $^{111}\text{In}$  solutes favor the Al site in spite of the larger space available at the  $R$  site indicates a predominance of the charge factor over the space factor which is consistent with the electronegativities of the elements involved (In: 1.78; Al: 1.61,  $R$ : 1.1–1.25; Pauling units). The tendency toward partial occupation of the

$R$  site at the end of the  $R$  series can be understood as a consequence of lanthanide contraction which—with increasing  $R$  atomic number—reduces the space available at the Al site and possibly also of the slight increase of the electronegativity from La to Lu. For a discussion of the temperature dependence of the Al-site occupation (Fig. 8) we refer to the work of Zacate and Collins.<sup>9</sup>

In  $RAI_3$  with cubic  $AuCu_3$  structure, the Al site has axial  $4/mmm$  point symmetry with 12 Al nearest neighbors at 0.297 nm (for  $a=0.42$  nm), and the  $R$  site has cubic point symmetry with 12 NN Al atoms at the same distance. From the observation of an axially symmetric QI of  $^{111}\text{Cd}$  we may conclude that in  $RAI_3$ ,  $R=\text{Tm, Yb, Lu}$  the  $^{111}\text{In}$  solutes prefer the Al over the  $R$  site which is not surprising, considering that both sites offer the same space.

Although the  $RAI_2$  samples contained only minute quantities ( $<5\%$ ) of  $RAI_3$ , the Al-site frequencies of  $RAI_3$ ,  $R=\text{Tm, Yb}$  were found to be predominant in the PAC spectra of the corresponding  $RAI_2$  compounds. This strong preference of the Al site of  $RAI_3$  over that of  $RAI_2$  is probably related to its larger size. This interpretation, however, does not explain why the  $RAI_3$  frequencies were only found in  $\text{TmAl}_2$  and  $\text{YbAl}_2$ , but not in  $\text{LuAl}_2$ .

In  $\text{TmAl}_2$  samples containing some  $\text{TmAl}_3$  ( $\leq 5\%$ ) we observed temperature-induced migration of the  $^{111}\text{In}$  solutes between the Al sites of  $\text{TmAl}_2$  and  $\text{TmAl}_3$  (see Fig. 7). The preference of the Al site of  $\text{TmAl}_3$  at low and that of  $\text{TmAl}_2$  at high temperatures is possibly due to differences in the lattice expansion of these compounds. To our knowledge, there are no experimental data on the variation of the  $RAI_3$  lattice parameter at high temperatures. The difference in the temperature dependence of the  $^{111}\text{Cd}$  quadrupole frequency in  $\text{TmAl}_2$  and  $\text{TmAl}_3$  (coefficients  $-d \ln \nu_q/dT=2.26$  and  $0.81 \times 10^{-4} \text{ K}^{-1}$ , respectively), however, suggests that in  $\text{TmAl}_2$  the thermal lattice expansion might be stronger than in  $\text{TmAl}_3$ . It is therefore conceivable that at high temperatures the Al site of  $\text{TmAl}_2$  offers the larger space for the solute atoms.

The fluctuating QI observed in  $RAI_3$ ,  $R=\text{Tm, Yb, Lu}$  at  $T > 800$  K can be attributed to diffusion jumps of the  $^{111}\text{In}$  probe atoms on the Al sublattice. Such jumps change the orientation, but not the magnitude of the EFG at the probe site. For details on the possible diffusion mechanisms we refer to the recent PAC study of  $^{111}\text{In}$  jumps in  $R\text{In}_3$  (Refs. 26–28) which has the same  $AuCu_3$  structure as  $RAI_3$ ,  $R=\text{Tm, Yb, Lu}$ . The activation enthalpies  $E_A=1.6(1)$  and  $1.2(1)$  eV for  $R=\text{Tm, Lu}$  and  $R=\text{Yb}$ , respectively, are of the same order as in the heavy  $R\text{In}_3$ . Since in the slow fluctuation regime  $\lambda_2=w$ , the temperature dependence of  $\lambda_2$  in Fig. 12 corresponds to attempt frequencies  $w_0=(1_{-0.5}^{+1}) \times 10^{14} \text{ s}^{-1}$  for  $R=\text{Tm, Lu}$  and  $w_0=(2.7_{-1.1}^{+1.7}) \times 10^{13} \text{ s}^{-1}$  for  $R=\text{Yb}$ . The jump frequencies in  $R\text{In}_3$  were found to depend sensitively on small deviations from the stoichiometric composition.<sup>26–28</sup> Slight composition differences are possibly responsible for the difference of the jump frequencies in  $RAI_3$ ,  $R=\text{Tm, Lu}$  and  $R=\text{Yb}$ .

The abrupt transition from total attenuation to an unperturbed correlation within 25–35 K in the high temperature PAC spectra of  $RAI_3$  (see Figs. 9 and 10) is most probably

not the result of a fast fluctuation process. Such an interpretation would require an unrealistically large activation enthalpy ( $E_A \sim 30$  eV) of the  $^{111}\text{Cd}$  diffusion at temperatures  $T > 1000$  K. More likely, the transition reflects a change in the site preference. The insert in Fig. 12 shows that at  $T > 1000$  K the  $^{111}\text{In}$  solutes tend to occupy the cubic  $R$  site with zero QI rather than the axial Al site which explains the observation of an unperturbed angular correlation at high temperatures.

## B. Electric field gradients in $RAI_2$ and $RAI_3$

### 1. Room temperature trends

We have extended the  $R$  dependence of the QI of  $^{111}\text{Cd}$  in  $RAI_2$  beyond the previous measurements by Mishra *et al.*<sup>5</sup> to include to  $R=\text{Tm, Yb, Lu}$ , and  $\text{Y}$  and have determined the  $^{111}\text{Cd}$  QI in  $RAI_3$ ,  $R=\text{Gd, Tm, Yb, and Lu}$ . The RT results are collected in Fig. 3. The bottom-most section shows the  $R$  dependence of the  $^{111}\text{Cd}$  quadrupole frequency in  $RAI_2$ , and the middle section the quadrupole frequencies of  $^{111}\text{Cd}$  in  $RX_3$  compounds with  $AuCu_3$  structure. Presently, data are available for  $X=\text{In, Sn}$  (Ref. 29) and Al (this investigation and Ref. 17).

In  $\text{EuAl}_2$  and  $\text{YbAl}_2$ , the room temperature QI of  $^{111}\text{Cd}$  deviates strongly from the general trend in the  $RAI_2$  series. The PAC spectrum of  $\text{EuAl}_2$  shows unambiguously that the frequency is about a factor of 5 smaller than for the other  $R$  constituents. For  $\text{YbAl}_2$  the identification of the quadrupole frequency of  $^{111}\text{Cd}$  on the Al site is slightly more difficult because of the partial occupation of the  $R$  site ( $\nu_q \leq 2$  MHz; Table II) and the pronounced preference for the Al site of  $\text{YbAl}_3$  ( $\nu_q=71.2$  MHz; Table II). If we rule out that in a two-phase  $\text{YbAl}_2/\text{YbAl}_3$  sample the  $^{111}\text{In}$  solutes completely avoid the Al site of  $\text{YbAl}_2$ , we may identify the 11 MHz component in the RT spectrum of  $\text{YbAl}_2$  as the quadrupole frequency of  $^{111}\text{Cd}$  on the Al site of this compound and conclude that the quadrupole frequencies of  $^{111}\text{Cd}$  in  $\text{EuAl}_2$  and  $\text{YbAl}_2$  are of the same order ( $\sim 10$  MHz).

The drastic decrease of  $\nu_q(^{111}\text{Cd}:RAI_2)$  at  $R=\text{Eu, Yb}$  relative to the other  $RAI_2$  can be attributed to the smaller valence of these  $R$  constituents which manifests itself also in an increase of the lattice constant  $a$  [compare  $\nu_q(^{111}\text{Cd}:RAI_2)$  and  $a(RAI_2)$  in Fig. 3]. The reduced QI of  $\text{YbAl}_2$  is consistent with the results of previous investigations<sup>30–33</sup> which indicate that the valence of Yb in  $\text{YbAl}_2$  is in an intermediate state with a value varying from 2.15 at low temperatures to 2.5 at 750 K. A similar behavior is found in  $R\text{In}_3$  and  $R\text{Sn}_3$  (Ref. 25): Here the  $^{111}\text{Cd}$  quadrupole frequency of  $R=\text{Eu}$  and  $\text{Yb}$  is a factor of 2–4 below the general trend in these  $AuCu_3$ -type compounds. The relation between the  $R$  valence and the QI of nuclear probes in  $RX_3$ ,  $X=\text{In, Sn}$  has been discussed by Schwartz and Shirley<sup>29</sup> in terms of a point charge model and by Asadabadi *et al.*<sup>34</sup> on the basis of *ab initio* calculations.

In  $RAI_3$ , however, there is practically no singularity of the lattice parameter at  $R=\text{Yb}$  (topmost section of Fig. 3; data from Ref. 17) and the  $^{111}\text{Cd}$  quadrupole frequency in  $\text{YbAl}_3$  is only about 15% smaller than in neighboring  $\text{TmAl}_3$  and

LuAl<sub>3</sub>. This observation is in fair agreement with a NMR measurement<sup>35</sup> of the quadrupole coupling constant of the probe <sup>27</sup>Al in TmAl<sub>3</sub> and YbAl<sub>3</sub>. From the small difference of the QIs of the neighboring RAl<sub>3</sub> and the continuous decrease of the lattice parameter we may infer that the valence of R=Yb in RAl<sub>3</sub> is close to that of R=Tm, Lu, i.e., almost 3+, which agrees with conclusions based on transport, thermodynamic, and magnetic data<sup>30,31,36</sup> that YbAl<sub>3</sub> may be considered an intermediate valence system with almost trivalent Yb ions.

In the trivalent RAl<sub>2</sub>, the RT quadrupole frequency of <sup>111</sup>Cd first increases with increasing R atomic number to reach a maximum at R=Ho, Er and then decreases by about 10% toward R=Lu (see Fig. 3). Wanting *ab initio* calculations of solute EFGs in RAl<sub>2</sub>, we compare this variation qualitatively to that of the EFG  $V_{zz}^{\text{latt}}$  produced by point charges on the lattice positions. In the point charge model (for a critical assessment see, e.g., Ref. 34) the quadrupole frequency is frequently written as:<sup>37</sup>  $\nu_q \propto Q(1-k)(1-\gamma_\infty)V_{zz}^{\text{latt}}$ , where  $(1-\gamma_\infty)$  is the Sternheimer correction and  $(1-k)$  an enhancement factor which accounts for the valence electron EFG and other contributions. In the present case of a cubic host lattice,  $V_{zz}^{\text{latt}}$  is proportional<sup>29</sup> to the inverse volume  $a^{-3}$  of the unit cell and therefore:  $\nu_q a^3 \propto Q(1-k)(1-\gamma_\infty)$ .

The quantity  $\nu_q a^3 \propto Q(1-k)(1-\gamma_\infty)$  varies—with a maximum at R=Ho—by about 25% across the series of trivalent RAl<sub>2</sub> (see dotted line in bottom section of Fig. 3). A similar trend has been observed in the hexagonal R metals.<sup>6</sup> Here too the enhancement factor  $(1-k)$  of the <sup>111</sup>Cd EFG increases in the first half and decreases in the second half of the R series.

Two mechanisms—one involving electron charge transfer from the solute atom to the R neighbors,<sup>38</sup> the other volume mismatch effects between impurity and host<sup>5</sup>—have been discussed with respect to the R dependence of the enhancement factor  $(1-k)$ . However, neither of these models provides a consistent explanation for the variation of  $\nu_q a^3$  across the RAl<sub>2</sub> series established in this study: While the volume mismatch of oversized <sup>111</sup>Cd on the Al site is expected to result in an increase of  $(1-k)$ , the charge transfer model predicts a continuous decrease of the enhancement factor with increasing R atomic number. The interpretation of the R dependence of the room temperature EFG of <sup>111</sup>Cd in trivalent RAl<sub>2</sub> thus remains an open question.

### C. Temperature dependence of the electricfield gradient in RAl<sub>2</sub> and RAl<sub>3</sub>

The temperature dependence of the EFG has been investigated for numerous probe nuclei in a large number of non-cubic metals<sup>39</sup> and in many intermetallic compounds. For non-R probe nuclei, the EFG usually decreases continuously with increasing temperature, in many cases following a  $T^{3/2}$  relation which has been attributed to the temperature-induced vibrations of the host atoms.<sup>40</sup> A recent review of the relevant literature on this subject has been given by Torumba *et al.*<sup>41</sup> in a paper reporting a first-principles calculation of the temperature dependence of the EFG in hcp Cd.

At R nuclei the dominant EFG contribution comes from the incomplete 4f shell. This contribution is proportional to

the thermal average of the 4f quadrupole moment over all crystal electric field (CEF) states and therefore strongly temperature dependent. As examples we cite the temperature variation of the QI of the Mössbauer (MS) isotope <sup>169</sup>Tm in TmCu<sub>2</sub> (Ref. 42) and in TmBa<sub>2</sub>Cu<sub>4</sub>O<sub>8</sub> (Ref. 43), of the MS nucleus <sup>174</sup>Yb in YbCu<sub>2</sub>Si<sub>2</sub> (Ref. 44) and of the PAC probe <sup>172</sup>Yb in Yb<sub>2</sub>Co<sub>3</sub>Ga<sub>9</sub> (Ref. 45).

The EFG of <sup>111</sup>Cd in the heavy RAl<sub>2</sub> decreases monotonously as temperature is raised (see the data of LuAl<sub>2</sub> and YAl<sub>2</sub> in Fig. 5 as examples), but the trend of  $\nu_q(T)$  is much closer to a linear function than a  $T^{3/2}$  relation. Similar relations have been reported for non-R probes in the hexagonal rare earth metals.<sup>7</sup> Here, too, the QI is to a very good approximation a linear function over a wide temperature range. However, while in RAl<sub>2</sub> the temperature coefficient  $-\frac{\delta \ln \nu_q(T)}{\delta T}|_{400 \text{ K}}$  is practically independent of the R constituent (see Tables I and II), the temperature dependence in the R metals shows a strong linear decrease with increasing R atomic number (Ref. 7) from  $-\frac{\delta \ln \nu_q(T)}{\delta T}|_{300 \text{ K}} \sim 12 \times 10^{-4} \text{ K}^{-1}$  for Nd to  $\sim 2 \times 10^{-4} \text{ K}^{-1}$  for Y.

In contrast to the heavy RAl<sub>2</sub>, the early members of the series (R=La-Sm) show a highly unusual temperature dependence of the QI for a closed shell probe nucleus: At  $T \geq 400 \text{ K}$  the EFG decreases with about the same slope as in the heavy RAl<sub>2</sub> (see Tables I and II), but at lower temperatures it passes through a maximum (Fig. 5). Apparently, the low temperature trend of the EFG at the Al site is affected by the properties of the 4f electrons. A mechanism which would account for this observation has been proposed by Rasera *et al.*:<sup>8</sup> The mechanism involves the overlap of the probe valence electrons with the 5d and 6s electrons of the rare earths which are hybridized by the interaction with the 4f shell. As consequence of this interaction, the nonspherical 4f charge distribution may be felt at neighboring lattice sites. The resulting 4f contribution to the EFG at the Al site would be important for light R with the stronger 5d (6s)–4f interaction caused by the larger radial extension of the 4f wave function<sup>46</sup> and would decrease with increasing temperatures due to the thermal averaging of the 4f quadrupole moment, with the details of the temperature variation depending on the parameters of the crystal electric field interaction. An interpretation of the experimental  $\nu_q(T)$  trends in Fig. 5 in terms of this mechanisms requires that the 4f and the lattice contributions to the EFG have opposite sign.

In the RAl<sub>3</sub> compounds with AuCu<sub>3</sub> structure, the temperature variation of the <sup>111</sup>Cd QI also varies with the R constituent (see Fig. 11): In YbAl<sub>3</sub> the quadrupole frequency passes through a shallow maximum while neighboring TmAl<sub>3</sub> and LuAl<sub>3</sub> show the same linear decrease with increasing temperature. The unusual temperature trend in YbAl<sub>3</sub> can be understood in terms of the noninteger Yb valence of this compound. The intermediate valence state is thought to result<sup>47</sup> from 4f charge fluctuations between two almost degenerate 4f configurations, trivalent Yb with 13 4f electrons, and divalent Yb with 14 4f electrons. Bauer *et al.*<sup>14</sup> have shown by Yb L<sub>III</sub> x-ray absorption measurements that with increasing temperature the relative weight of Yb<sup>3+</sup> (4f<sup>13</sup>) grows at the expense of Yb<sup>2+</sup> (4f<sup>14</sup>). The PAC time window is much longer than the valence fluctuation time. In

contrast to x-ray absorption, where both configurations are seen, PAC experiments therefore sample the time average of the two configurations. The QI at non- $R$  solutes in compounds with trivalent  $R$  constituents is larger than in the corresponding divalent compound (see Fig. 3). The time average of the  $^{111}\text{Cd}$  QI therefore increases with increasing weight of  $\text{Yb}^{3+}$  which explains the initial increase of  $\nu_q(^{111}\text{Cd}:\text{YbAl}_3)$  as temperature is raised from  $T=10$  K. At  $T>400$  K, the effects of lattice vibrations and lattice expansion overcome the growing weight of  $\text{Yb}^{3+}$  and the QI begins to decrease with increasing temperature.

## V. SUMMARY

We have investigated static and fluctuating EFGs experienced by the nuclear probe  $^{111}\text{In}/^{111}\text{Cd}$  on the Al site of the rare earth–aluminium compounds  $\text{RAl}_2$  and  $\text{RAl}_3$  as a function of temperature for different  $R$  constituents.

An anomalous temperature dependence of the EFG in the early  $\text{RAl}_2$  members suggests a substantial influence of the

$4f$  electrons on the EFG at the Al site. The temperature dependence in the intermediate valence compound  $\text{YbAl}_3$  is consistent with an increase of the  $4f$  hole occupation with temperature.

The measurements establish the site preference of  $^{111}\text{In}/^{111}\text{Cd}$  solutes in two-phase samples containing  $\text{RAl}_2$  and  $\text{RAl}_3$  and provide evidence for temperature-induced solute migration between these phases. Information on diffusion jumps of the solutes on the Al sublattice could be extracted by analyzing the nuclear spin relaxation observed at high temperatures in  $\text{RAl}_3$ ,  $R=\text{Tm}$ ,  $\text{Yb}$ , and  $\text{Lu}$ .

## ACKNOWLEDGMENTS

The authors gratefully acknowledge financial support by Deutscher Akademischer Austauschdienst (DAAD), Germany. The x-ray characterization of the  $\text{RAl}_3$  compounds has been carried out by H. Euler at Mineralogisch-Petrologisches Institut, University of Bonn.

\*Author to whom correspondence should be addressed; forker@iskp.uni-bonn.de

†Present address: Instituto de Magnetismo Aplicado, P.O. Box 155, 28230 Las Rozas, Madrid, Spain.

<sup>1</sup>R. G. Barnes, in *Handbook of Chemistry and Physics of Rare-Earths*, edited by K. A. Gschneidner and L. Eyring (North-Holland, Amsterdam, 1979), Vol. 2, Chap. 18.

<sup>2</sup>K. H. J. Buschow, in *Ferromagnetic Materials*, edited by E. P. Wohlfarth (North-Holland, Amsterdam, 1980), Vol. 1, Chap. 4.

<sup>3</sup>P. de la Presa, M. Forker, J. Th. Cavalcante, and A. P. Ayala, *J. Magn. Magn. Mater.* **306**, 292 (2006).

<sup>4</sup>M. Forker, P. de la Presa, M. Olzon-Dionysio, and S. Dionysio de Souza, *J. Magn. Magn. Mater.* **226-230**, 1156 (2001).

<sup>5</sup>S. N. Mishra, R. G. Pillay, K. Raghunathan, P. N. Tandon, S. H. Devare, and H. G. Devare, *Phys. Lett.* **91A**, 193 (1982).

<sup>6</sup>K. A. Gschneidner and V. K. Pecharsky, *Z. Kristallogr.* **221**, 375 (2006).

<sup>7</sup>M. Forker, L. Freise, and D. Simon, *J. Phys. F: Met. Phys.* **18**, 823 (1988).

<sup>8</sup>R. L. Rasera, B. D. Dunlap, and G. K. Shenoy, *Phys. Rev. Lett.* **41**, 1188 (1978).

<sup>9</sup>M. O. Zacate and G. S. Collins, *Phys. Rev. B* **69**, 174202 (2004).

<sup>10</sup>M. O. Zacate and G. S. Collins, *Phys. Rev. B* **70**, 024202 (2004).

<sup>11</sup>M. O. Zacate, B. C. Walsh, L. S.-J. Peng, and G. S. Collins, *Hyperfine Interact.* **136/137**, 653 (2001).

<sup>12</sup>P. Wodniecki, B. Wodniecka, A. Kulińska, M. Uhrmacher, and K. P. Lieb, *Hyperfine Interact.* **158**, 339 (2004).

<sup>13</sup>K. H. J. Buschow, M. Campagna, and G. K. Wertheim, *Solid State Commun.* **24**, 253 (1977).

<sup>14</sup>E. D. Bauer, C. H. Booth, J. M. Lawrence, M. F. Hundley, J. L. Sarrao, J. D. Thompson, P. S. Riseborough, and T. Ebiara, *Phys. Rev. B* **69**, 125102 (2004).

<sup>15</sup>J. H. N. van Vucht and K. H. J. Buschow, *Philips Res. Rep.* **19**, 319 (1964).

<sup>16</sup>A. M. van Diepen, K. H. J. Buschow, and H. W. de Wijn, *J.*

*Chem. Phys.* **51**, 5259 (1969).

<sup>17</sup>A. V. Tsvyashchenko, L. N. Fomicheva, V. B. Brudanin, O. I. Kochetov, A. V. Salamatina, A. Velichkov, M. Wiertel, M. Budzynski, A. A. Sorokin, G. K. Ryasny, and B. A. Komissarova, *Solid State Commun.* **142**, 664 (2007).

<sup>18</sup>M. Forker, W. Herz, U. Hütten, M. Müller, R. Müßeler, J. Schmidberger, D. Simon, A. Weingarten, and S. C. Bedi, *Nucl. Instrum. Methods Phys. Res. A* **327**, 456 (1993).

<sup>19</sup>H. Frauenfelder and R. M. Steffen, in *Perturbed Angular Correlations*, edited by K. Karlsson, E. Matthias, and K. Siegbahn (North-Holland, Amsterdam, 1963).

<sup>20</sup>M. Blume, *Phys. Rev.* **174**, 351 (1968).

<sup>21</sup>H. Winkler and E. Gerdau, *Z. Phys.* **262**, 363 (1973).

<sup>22</sup>A. Baudry and P. Boyer, *Hyperfine Interact.* **25**, 803 (1987).

<sup>23</sup>M. Forker, W. Herz, and D. Simon, *Nucl. Instrum. Methods Phys. Res. A* **337**, 534 (1993).

<sup>24</sup>U. Häussermann, S. Amerioun, L. Eriksson, C. S. Lee, and G. J. Miller, *J. Am. Chem. Soc.* **124**, 437 (2002).

<sup>25</sup>J. C. Slater, *J. Chem. Phys.* **41**, 3199 (1964).

<sup>26</sup>M. O. Zacate, A. Favrot, and G. S. Collins, *Phys. Rev. Lett.* **92**, 225901(E) (2004).

<sup>27</sup>G. S. Collins, A. Favrot, L. Kang, E. R. Niewenhuis, D. Solodovnikov, J. Wang, and M. O. Zacate, *Hyperfine Interact.* **159**, 1 (2004).

<sup>28</sup>G. S. Collins, A. Favrot, L. Kang, D. Solodovnikov, and M. O. Zacate, *Defect Diffus. Forum* **237-240**, 195 (2005).

<sup>29</sup>G. Schwartz and D. Shirley, *Hyperfine Interact.* **3**, 67 (1977).

<sup>30</sup>A. Iandelli and A. Palenzona, *J. Less-Common Met.* **29**, 239 (1972).

<sup>31</sup>E. E. Havinga, K. H. J. Buschow, and H. J. Van Daal, *Solid State Commun.* **13**, 621 (1973).

<sup>32</sup>A. Percheron-Guégan, J. C. Achard, O. Gorochev, F. Gontales-Jimenez, and P. Imbert, *J. Less-Common Met.* **37**, 1 (1974).

<sup>33</sup>S.-J. Oh, J. W. Q. Allen, M. S. Torikachvili, and M. B. Maple, *J. Magn. Magn. Mater.* **52**, 183 (1985).

- <sup>34</sup>S. J. Asadabadi, S. Cottenier, H. Akbarzadeh, R. Saki, and M. Rots, *Phys. Rev. B* **66**, 195103 (2002).
- <sup>35</sup>H. W. de Wijn, A. M. Van Diepen, and K. H. J. Buschow, *Phys. Rev. B* **1**, 4203 (1970).
- <sup>36</sup>A. Hiess, J. X. Bouvherle, F. Givord, J. Schweizer, E. Lelièvre-Berna, F. Tasset, B. Gillon, and P. C. Canfield, *J. Phys.: Condens. Matter* **12**, 829 (2000).
- <sup>37</sup>R. Raghavan, E. Kaufmann, and P. Raghavan, *Phys. Rev. Lett.* **34**, 1280 (1975).
- <sup>38</sup>M. Forker and W. Steinborn, *Phys. Rev. B* **20**, 1 (1979).
- <sup>39</sup>R. Vianden, *Hyperfine Interact.* **35**, 1079 (1987).
- <sup>40</sup>K. Nishiyama and D. Riegel, *Hyperfine Interact.* **4**, 490 (1978).
- <sup>41</sup>D. Torumba, K. Parlinski, M. Rots, and S. Cottenier, *Phys. Rev. B* **74**, 144304 (2006).
- <sup>42</sup>P. C. M. Gubbens, K. H. J. Buschow, M. Divis, M. HeideIman, and M. Loewenhaupt, *J. Magn. Magn. Mater.* **104-107**, 1283 (1992).
- <sup>43</sup>G. A. Stewart, S. J. Harker, and D. M. Pooke, *J. Phys.: Condens. Matter* **10**, 8269 (1998).
- <sup>44</sup>V. Zevin, G. Zwicknagl, and P. Fulde, *Phys. Rev. Lett.* **60**, 2331 (1988).
- <sup>45</sup>S. K. Dhar, C. Mitra, P. Bonville, M. Rams, K. Królas, C. Godart, E. Alleno, N. Suzuki, K. Miyake, N. Watanabe, Y. Onuki, P. Manfrinetti, and A. Palenzona, *Phys. Rev. B* **64**, 094423 (2001).
- <sup>46</sup>A. J. Freeman and J. P. Desclaux, *J. Magn. Magn. Mater.* **12**, 11 (1979).
- <sup>47</sup>J. M. Lawrence, P. S. Riseboroughs, and R. D. Parks, *Rep. Prog. Phys.* **44**, 1 (1981).